Enhancement of trace gas detection by integrating wavelength modulated spectra across multiple lines

Andreas Karpf and Gottipaty N. Rao*

Department of Physics, Adelphi University, Garden City, New York 11530, USA

*Corresponding author: rao@adelphi.edu

Received 29 October 2009; revised 27 January 2010; accepted 5 February 2010; posted 17 February 2010 (Doc. ID 119224); published 8 March 2010

We describe and demonstrate a technique that enhances the sensitivity of a spectrometer for trace gas detection by employing wavelength modulation spectroscopy (WMS) and integrating the absolute value of the recorded spectra across multiple lines of the species. The sensitivity is further enhanced by conducting WMS with large modulation depths. This technique is demonstrated using a continuously tunable external cavity CW quantum cascade laser to record the second harmonic wavelength modulated spectra of NO_2 across the peak of the R-branch from 1629.5 to 1633.9 cm^{-1}. By integrating the absolute value of the resulting spectra, the detection sensitivity of NO_2 is improved by a factor of 40 compared to the sensitivity achieved using single-line WMS with the same apparatus. By using this technique, we achieve a sensitivity of approximately 6 parts in 10^9 (ppb) using a short-path cell (a 1 m absorption cell with two passes).

OCIS codes: 000.2170, 010.1120, 120.6200, 280.3420, 300.6340.

1. Introduction

The real-time detection of trace amounts of contaminants and pollutants in the atmosphere is of great interest to a wide range of fields, including environmental science, safety monitoring, air quality control (e.g., for compliance with Environmental Protection Agency regulations [1]), defense and homeland security (e.g., for the detection of trace amounts of explosives or explosive components [2]), and medical diagnostics [3]. In these applications, the concentrations of pollutants typically range from several parts per million (ppm) to the parts in 10^{12} (ppt) level and thus require techniques that are both highly sensitive and selective. Nitrogen oxides (NO_x) are of particular interest since they are some of the most damaging of these pollutants. They play important roles in the formation of photochemical smog, the formation of tropospheric ozone, and the formation of acid rain, and thus can directly impact public health.

Laser-based techniques for trace gas detection have many advantages over other techniques because of their ability to provide real-time monitoring capabilities with greater sensitivity and selectivity. In particular, quantum cascade lasers are attractive sources for trace gas detection because they operate in the mid-infrared region ($\lambda = 4$ to $24\,\mu$m) and thus provide access to the fundamental rotational–vibrational transitions of molecular species [4,5]. This offers improved sensitivity of several orders of magnitude over near-infrared diode-laser-based techniques that employ the detection of the overtones of the molecular transitions. Quantum cascade lasers have been used to detect several trace gasses (e.g., CO, CO_2, NO, NO_2, NH_3, CH_4, and N_2O) with different spectroscopic techniques (e.g., laser absorption spectroscopy, cavity ringdown spectroscopy, integrated cavity output spectroscopy) as described in the review article by Tittel *et al.* [5]. By employing an external cavity arrangement, a quantum cascade laser offers a narrow linewidth ($\Delta\nu \sim 0.001\,cm^{-1}$), highly stable and reproducible tunable CW output, and a wide continuous tuning range, all of which

0003-6935/10/081406-08$15.00/0

are essential for the study of complex spectra, as is the case in investigating trace gas components in the atmosphere [6,7].

Laser absorption spectroscopy is based on recording the change in intensity of laser radiation as it passes through a region containing the sample of interest. As the laser is tuned across a transition, the transmitted laser intensity is a function of frequency ν given by Beer's law:

$$I(\nu) = I_0(\nu)e^{-\alpha(\nu)L}, \tag{1}$$

where I_0 is the incident laser intensity, L is the optical path length, and $\alpha(\nu)$ is the absorption coefficient at frequency ν [8]. In the low-concentration regime (where $\alpha(\nu)L \le 0.05$), one can approximate Eq. (1) as

$$I(\nu) = I_0(\nu)[1 - \alpha(\nu)L]. \tag{2}$$

When using laser absorption spectroscopy, the sensitivity of a spectrometer is often determined by taking the ratio of the amplitudes of the absorption line to that of the noise level.

The sensitivity of a laser-based sensor may be enhanced by using frequency modulation techniques. As the laser is slowly scanned across a transition, it is also modulated at a higher frequency (f) and detection is done at higher harmonics of the frequency (e.g., $2f$). This is done so that (i) low-frequency drifts in laser intensity do not affect the absorption measurements and (ii) excess laser noise, which varies as $1/f$, is reduced, thereby enhancing the signal-to-noise ratio. One characterizes these techniques as either frequency modulation (FM) or wavelength modulation spectroscopy (WMS), based on the frequency at which the laser is modulated. Specifically, FM spectroscopy is when the laser is modulated at frequencies greater than the absorption line width, while WMS is when the modulation frequencies are lower than the absorption line width [8,9]. The work reported in this paper makes use of WMS, where the sinusoidal modulation of the laser has a frequency in the tens of kilohertz; this is much less than the linewidth of the NO_2 transitions with which we worked (linewidth $\sim$900 MHz(0.03 cm^{-1}) at a pressure of 110 mbar).

The modulated laser frequency may be expressed as

$$\nu(t) = \bar{\nu} + a\cos(\omega t), \tag{3}$$

where $\bar{\nu}$ is the mean laser frequency as it is slowly scanned, a is the amplitude of the modulation, and ω is the angular frequency of the modulation. If the tuning range and modulation amplitude a are small, then one may treat the incident laser intensity $I_0(\nu)$ as constant (this is typically the case for tunable diode lasers, as well as for the external cavity quantum cascade laser used in the present work). As a result, Eq. (2) may be rewritten as

$$I(\nu) = I_0(\nu)[1 - \alpha(\bar{\nu} + a\cos\omega t)L]. \tag{4}$$

The time-dependent term above can be expanded as a cosine Fourier series:

$$\alpha(\bar{\nu} + a\cos\omega t) = \sum_{n=0} H_n(\bar{\nu})\cos n\omega t, \tag{5}$$

where $\bar{\nu}$ is considered to be constant over a modulation period. $H_n(\bar{\nu})$ is the nth Fourier component of the modulated absorption coefficient. Using a lock-in amplifier, one can detect the nth harmonic of the modulation frequency. This provides a means to measure the absorption since the processed signal of the nth harmonic is proportional to $I_0H_n(\bar{\nu})L$, where $H_n(\bar{\nu})$ itself is proportional to the absorption coefficient α. If the modulation amplitude a is small enough, the nth Fourier amplitude is proportional to the nth derivative of the absorption signal [8]:

$$H_n(\bar{\nu}) = \frac{2^{n-1}}{n!}a^n \frac{d^n\alpha(\nu)}{d\nu^n}\bigg|_{\nu=\bar{\nu}}. \tag{6}$$

When using WMS, the sensitivity of a spectrometer is often determined by taking the ratio of the peak-to-peak amplitude of the WMS signal of an absorption line to that of the noise level.

Using an absorption line's amplitude to detect a species, however, neglects the width of the line and, as a result, gives the same intensity for both broad and narrow lines with the same amplitude. For example, even though a 25 ppm sample of NO_2 at 600 mbar has 12 times more molecules than the same sample at 50 mbar, its absorption spectrum shows only about a 25% enhancement in peak absorption: The majority of additional absorption manifests itself in the broadening of the lines [10,11]. As a result, when dealing with broadened lines, a more accurate measure of the absorption intensity can be achieved by integrating over the absorption line. Assuming that the absorbance $a = \alpha(\nu)L$ is small (as is typically the case with trace gas detection), the integrated absorption may be written as

$$S = \int \alpha(\nu)L\mathrm{d}\nu. \tag{7}$$

Since the absorption coefficient $\alpha(\nu) = \sigma(\nu)N$, where $\sigma(\nu)$ is the cross section and N is the concentration, the integrated absorption signal for a single line is proportional to the concentration of the species. Based on this, it has been shown that the sum of the areas of a set of absorption lines varies linearly with the concentration, and conducting trace gas detection by integrating multiple absorption lines can enhance the sensitivity of a detector by over 1 order of magnitude [11].

This concept may be extended to further enhance the sensitivity of a detector by integrating the absolute value of the wavelength modulation spectra of a species over multiple lines. Since the nth Fourier amplitude $H_n(\bar{\nu})$ is proportional to the absorption coefficient α, integrating the absolute value of the

WMS signal yields a result that is also proportional to the concentration. Thus, integrating the absolute value of the WMS signal over multiple lines for a species yields a sensitivity comparable to using standard absorption or WMS techniques over a much longer path length. The effective path length depends on the number of transitions employed and their absorption characteristics. If the target species has a dense set of rotational-vibrational states (e.g., NO_2), the multiple-line integrated signal could contain the contribution of dozens or even hundreds of lines and reach an effective path length of several hundred meters. Multiple-line integrated spectroscopy has the added advantage that saturation and line-broadening effects can be minimized compared to long path absorption and WMS techniques.

It should be noted that higher harmonic detection involves higher-order derivatives of the absorption lines [9]. The absorption lines may be represented by Voigt profiles, resulting in derivatives that have both positive and negative parts. When integrating, the contributions from the positive and negative parts effectively cancel. However, since the absolute value of the nth Fourier amplitude is proportional to the concentration, we take the absolute value of both parts of the signal and sum over all of the absorption features.

The integrated WMS signal for a particular concentration may be maximized by preparing the sample at an optimal pressure. The optimal pressure for laser absorption techniques, such as tunable diode laser absorption spectroscopy is in the 10–50 mbar range, which provides the best balance between sensitivity and selectivity [10]. The multiple-line integrated absorption signal was enhanced by preparing the samples at a higher pressure (e.g., 600 mbar) [11]. This is because pressure-broadening increased the area enclosed by the absorption lines. As seen from Eq. (6), however, the WMS signals are proportional to the derivatives of the absorption lines. As a result, pressure-broadened absorption lines will have shallower slopes and, thus, weaker WMS signals. The optimal pressure for an integrated WMS signal is a balance between achieving the steep slopes seen in absorption lines at low pressures, and in the increased number of molecules present at higher pressures. This was determined for NO_2 by generating a simulated absorption spectrum for several different pressures, taking the second derivative of the simulation, and then integrating the results across a desired spectral range (in this case, over the peak of the NO_2 R-band described below in Section 2). The amplitude of the integrated signal versus pressure was plotted (see Fig. 1), and the optimal pressure was determined to be approximately 100 mbar. The simulation was generated using the HITRAN database [12] and the SPECTRA software developed by Mikhailenko *et al.* [13].

The area under the WMS signals may be enhanced by using a large modulation amplitude a. It has been shown that the peak-to-peak amplitude of a second

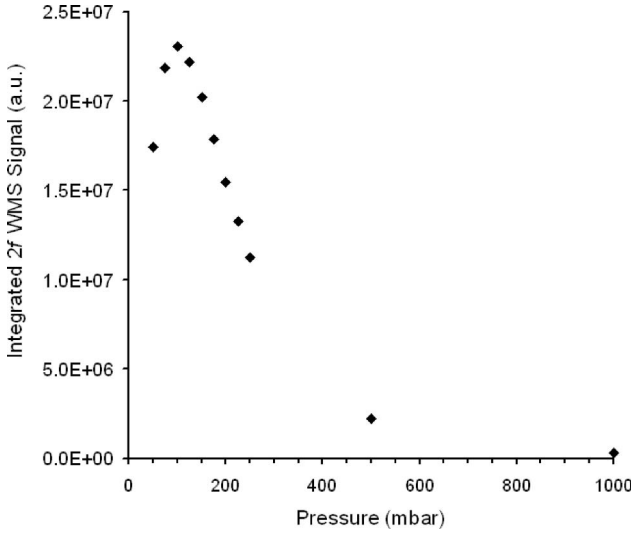

Fig. 1. Plot of the integrated second harmonic ($2f$) wavelength modulation spectra versus pressure generated from simulated spectra based on the HITRAN database [12]. The peak value of the signal occurs at a pressure of about 100 mbar.

harmonic WMS signal is maximized when the modulation amplitude $a = 2.2\Delta\nu$, where $\Delta\nu$ is the half-width at half-maximum for the corresponding absorption line [8]. At larger modulation amplitudes, the peak-to-peak amplitude of a second harmonic WMS signal slowly decreases (for a Voigt line profile, it reduces to 80% of its peak value at $a = 5\Delta\nu$). However, at large modulation amplitudes, there is an associated increase in the linewidth, leading to a broadening of the WMS signal [14]. This broadening leads to a larger integrated area of the absolute value of the second harmonic WMS signal.

In the case of large modulation amplitudes, when one modulates the laser using injection current tuning (as is the case with tunable diode lasers, as well as the quantum cascade laser used in the present work), the incident laser intensity $I_0(\nu)$ can no longer be treated as constant: the laser's intensity, as well as its frequency, will be simultaneously modulated. Equation (3) may be rewritten to take this into account [15]:

$$\nu(t) = \bar{\nu} + a\cos(\omega t + \psi), \tag{8}$$

where ψ is the phase shift between the intensity modulation (IM) and the FM. The resulting laser intensity may be written as [16]

$$I_0(t) = \bar{I}_0[1 + i_0\cos(\omega t + \psi_1) + i_2\cos(2\omega t + \psi_2)], \tag{9}$$

where $\bar{I}_0$ is the average laser intensity at $\bar{\nu}$, the first cosine term is the first harmonic ($1f$) term, i_0 is the linear ($1f$) IM amplitude, ψ_1 is the FM/IM phase shift, the second cosine term is the second harmonic ($2f$) term, i_2 is the nonlinear ($2f$) IM amplitude (both i_0 and i_2 are normalized by $\bar{I}_0$), and ψ_2 is the phase shift of the nonlinear IM.

For the larger tuning and modulation amplitudes involved, Eq. (2) must be rewritten to include contributions from multiple lines:

$$I(\nu) = I_0(\nu)[1 - \alpha(\nu)L] = I_0(\nu)[1 - P\chi_i L\sum_j S_j\varphi_j], \quad (10)$$

where P is the total gas pressure (in atmospheres), χ_i is the mole fraction of the ith absorbing species (there is an implied summation over the i component species in the case of multiple species in a gas sample), and S_j and φ_j are, respectively, the line strength and line shape of the jth feature. The summation takes into account the overlap of adjacent features. When modulated, the spectral absorbance $\alpha(\bar{\nu} + a\cos\omega t)$ may still be expanded as a Fourier series:

$$-\alpha(\bar{\nu} + a\cos\omega t) = \sum_{n=0} H_n(\bar{\nu}, a)\cos n\omega t, \quad (11)$$

where the nth Fourier component of the modulated absorption coefficient is

$$H_n(\bar{\nu}, a) = -\frac{P\chi_i L}{2\pi}\int_{-\pi}^{\pi}\sum_j S_j\varphi_j(\bar{\nu} + a\cos\theta)\cos k\theta \mathrm{d}\theta. \quad (12)$$

As in the case with small modulation amplitude, H_n is proportional to concentration. Li *et al.* [16] show that the X and Y components of the lock-in signal for $2f$ detection are

$$X_{2f} = \frac{G\bar{I}_0}{2}\left[H_2 + \frac{i_0}{2}(H_1 + H_3)\cos\psi_1 + i_2\left(1 + H_0 + \frac{H_4}{2}\right)\cos\psi_2\right], \quad (13)$$

$$Y_{2f} = -\frac{G\bar{I}_0}{2}\left[\frac{i_0}{2}(H_1 - H_3)\sin\psi_1 + i_2\left(1 + H_0 - \frac{H_4}{2}\right)\sin\psi_2\right]. \quad (14)$$

The absolute magnitude of the $2f$ signal is

$$R_{2f} = \sqrt{X_{2f}^2 + Y_{2f}^2}. \quad (15)$$

If the laser tuning and modulation parameters are kept the same between successive scans of different concentrations of a species, then, since the H_n are proportional to the sample concentration, so is the recorded $2f$ signal from the lock-in amplifier. This, in turn, means that the signal recorded by integrating the absolute value of the wavelength modulation spectra of a species over multiple lines using large modulation amplitudes will be proportional to the concentration of the target species.

We define the integrated second harmonic WMS signal W_T as a new experimental parameter and measure it for different concentrations of the target species. As a result, by using precalibrated reference mixtures of the desired gas, one can define a W_T versus concentration curve that characterizes a particular experimental apparatus (e.g., this would take into account the optical path length L, the tuning range, the modulation amplitude, and other equipment-related factors). One could then identify the unknown concentrations of the species by recording their W_T and identifying their corresponding positions on this chart.

Monitoring trace gases in the atmosphere is a complex process because they often depend on local industrial, environmental, meteorological, and other conditions. One should carefully look at the constituents of the local atmosphere for any contributions from other trace gases to the absorption spectra. The possible contributions from other trace species may be addressed either by choosing an appropriate spectral region for the absorption measurements (as described for the detection of NO_2 in Section 2), or by subtracting off their corresponding contribution.

Integrating the wavelength modulated spectra across multiple lines should enhance the sensitivity of detection in two ways. The first enhancement would be due to the summing of the area under the absolute value of the WMS signal recorded for many spectral lines (which would boost the magnitude of the recorded signal). The second enhancement is from the fact that the integration has the effect of averaging the random components of the noise. Because these data are acquired in a single scan, this effective averaging of the noise occurs in a much shorter time span compared to adding the data of repeated scans. The data acquisition rates for multiple-line integrated spectroscopy are expected to be significantly less than the multiple scans and summation procedures often employed for trace gas detection [11]. This is likely to be an advantage for real-time applications in the study of chemical reactions in the atmosphere and in breath analysis. This procedure is particularly valuable for molecules that have a large number of transitions grouped together.

2. Experimental Details

We carried out WMS of NO_2, using a short-path absorption cell (1 m) filled with different concentrations of NO_2 (5, 2.5, 1, 0.5, and 0.25 ppm). The schematic of the experimental arrangement is shown in Fig. 2. The quantum cascade laser output is split into two beams by using a 50/50 beam splitter; one beam is directed to the experimental cell and the other passes through a reference cell. Rectangular, flat, protected gold mirrors were aligned to reflect the beams back through each cell and then direct the returning beams to their corresponding detectors. This

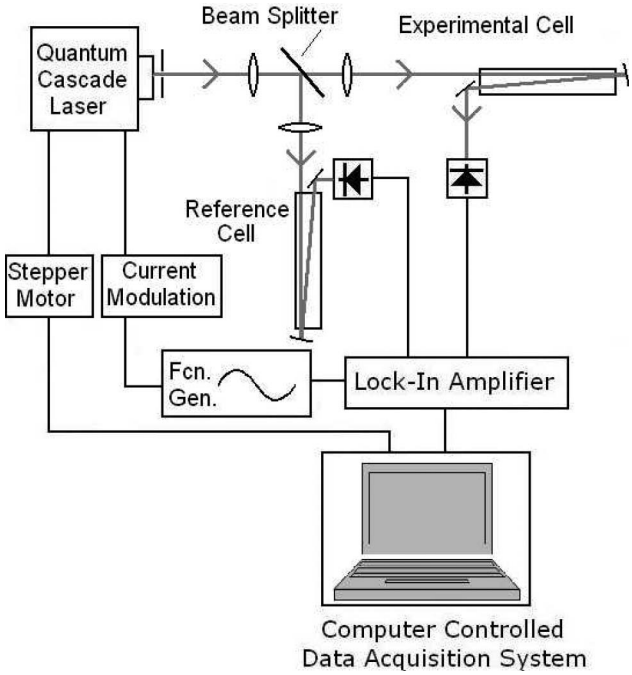

Fig. 2. Schematic of the experimental setup used for WMS of NO_2.

results in an effective path length of 2 m through the experimental cell. Detection of the exiting beams was done using two-stage, TE-cooled, IR photovoltaic detectors (PVI-2TE-8 manufactured by Vigo), which can be operated in a room-temperature environment. The detectors were optically immersed in a high refractive index, hyperhemispherical lens.

The quantum cascade laser source was purchased from Daylight Solutions (model TLS-CW-MHF) and has a tuning range of 1601.3 to 1670 cm^{-1}. The external cavity is of a Littrow configuration, which allows a wide range of mode-hop-free tuning, provides a narrow linewidth ($\sim$0.001 cm^{-1}), and is thus well suited for spectroscopic measurements. The laser tuning was monitored using an etalon and the laser controller's display screen, as well as by comparing recorded spectra with line positions identified in the HITRAN database [12]. The laser power varies as a function of tuning, with a minimum output power of 14 mW at 1601.3 cm^{-1}, and a maximum of 21 mW at 1640.4 cm^{-1}. The output power at 1630 cm^{-1} (the frequency at which we conducted WMS) was 19.5 mW. The minimum spot size of the beam is approximately 2 mm. Broad range tuning is achieved entirely by rotating the external cavity grating via a stepper motor; no current or temperature tuning was necessary. The system may be set to one of six preset tuning rates, the slowest of which was 3.125 cm^{-1}/s (the tuning rate used to record our NO_2 spectra). The sinusoidal modulation used for WMS was generated by feeding a 45 kHz, 5 V_{pp} sine wave (generated using a Stanford Research Systems DS 345 function generator) to the current modulation input on the laser head. The 5 V_{pp} sine wave (the maximum that may be used with the Daylight Solutions quantum cascade laser) corresponds to a modulation amplitude of $a = 7\Delta\nu$ (for NO_2 at a pressure of 110 mbar $\Delta\nu \sim .012\ cm^{-1}$).

The output from each detector was fed to a lock-in amplifier (Stanford Research Systems SR830 DSP). The lock-in time constant was set to 3 ms. The signal from each lock-in was fed into a separate channel on a National Instruments (model PCI-6040E) data acquisition board. A virtual instrument constructed using LabVIEW for Windows was used to record the data. The signals from the sample cell and reference cell were subtracted during data processing on the personal computer.

The NO_2 mixtures were prepared by loading the experimental cell with a precalibrated mixture of NO_2 in zero air (a mix of 20.9% O_2 and 79.1% N_2). The precalibrated NO_2 mixture had a concentration of 5 ppm and was certified by Gasco Affiliates, LLC, to $\pm 10\%$ of the specified concentration. Other concentrations used in the experiment were created by loading the cell with the 5 ppm mixture to a certain pressure, and then adding zero air to increase the pressure to the desired final value (110 mbar). For example, the 1 ppm concentration was generated by first loading the experimental cell with 22 ± 2 mbar of the precalibrated 5 ppm mix of NO_2 before additional zero air was added to reach a final pressure of 110 ± 10 mbar. Because of limitations in the accuracy of our vacuum/mixing apparatus, the concentrations prepared are expected to be accurate to $\pm 15\%$ (e.g., the 1 ppm concentration mixture is expected to contain between 0.85 and 1.15 ppm NO_2). The mixing apparatus was tested by generating several concentrations of NO_2 and comparing the recorded absorption line intensities with the calculated intensities based on HITRAN [12]. This confirmed that the mixtures were within the expected uncertainty.

Experiments in the mid-infrared and far infrared typically suffer from significant etalon effects. We identified etalonning in our signal due to a beam splitter. The etalon effects from the beam splitter were removed by placing it between the lenses of a 2× beam expander ($f_1 = 25.8$ mm, $f_2 = 50.6$ mm); the short focal lengths were necessary to create enough divergence to remove the etalon peaks. Wedge windows (antireflection coated ZnSe with faces that were 1° away from parallel) were used in the cell to remove etalonning that occurs with standard, parallel-faced windows. The quantum cascade laser itself exhibited etalonning due to its antireflection coatings. We compensated for this by subtracting empty-cell scans of the laser (which characterized the tuning characteristics of the laser, including etalonning) from scans of the cell loaded with NO_2.

To integrate the recorded spectra for multiple lines over a desired range of frequencies, the laser source must tune without mode hops across that range. The quantum cascade laser used in this experiment was capable of mode-hop-free tuning between 1603.5 and 1670 cm^{-1}. This provided access to half of the NO_2

P-branch and the entire NO_2 R-branch (the peak absorption in the R-branch occurs at 1630.3 cm^{-1}). The next consideration was to select a region with a strong dense spectrum that is free from interference due to other species. A review of the component species present in the atmosphere and the species included in the HITRAN database [12,17] showed that only H_2O and NH_3 have transitions in the region of interest that were potentially strong enough to cause interference. However, the effects of NH_3 could be ignored due to the fact that the expected concentration of NH_3 in ambient air (away from significant forest, industry, or farm sources) is in the 100 ppt–10 ppb range [18,19], and the fact that the NH_3 transitions are over 2 orders of magnitude weaker than the corresponding NO_2 transitions. The strength of the water lines, however, necessitated that we select a region in which they did not significantly interfere with recording NO_2 spectra. Figure 3(a) shows a simulated spectrum illustrating the regions where the water lines (due to ambient water vapor in the beam path leading to the experimental cell) overlap and thus overwhelm any potential signal from the NO_2 R-branch. This simulation was generated using the HITRAN database [12] and the SPECTRA software developed by Mikhailenko *et al.* [13]. We have not directly accounted for water vapor continuum absorption effects. However, it should be stated that the effect of the continuum on the WMS signals, which are derivatives of the absorption data, is expected to be small. This is corroborated by the fact that the line positions and line intensities calculated using the HITRAN data agreed well with the reported experimental results. The strength of the water lines was selected to match typical conditions in the mid-latitude U.S. during the summer months (the water vapor density used was 14.97 g/m^3, which corresponds to a relative humidity of 71% at 23 °C, and is the average humidity in Washington, D.C., in July) [20]. From Fig. 3, one would notice that the region between the water lines at 1627.82 and 1634.97 cm^{-1} proves to be the longest continuous region in which absorption due to the water lines does not overwhelm the NO_2 lines, and covers the peak of the R-branch. Because of the broad width of these water lines and limitations in our apparatus, our ability to record continuous second harmonic WMS NO_2 signals was limited to the region between 1629.5 and 1633.9 cm^{-1}. It is important to note that this tuning range covered over 400 NO_2 transitions, of which approximately 20% may be considered relatively strong (i.e., having transition strengths over 10% that of the strongest transition in the R-branch). It should also be noted that the strength and width of the water lines in the simulation were calibrated to match our experimental apparatus (which had a roughly 1 m path from the laser to the experimental cell).

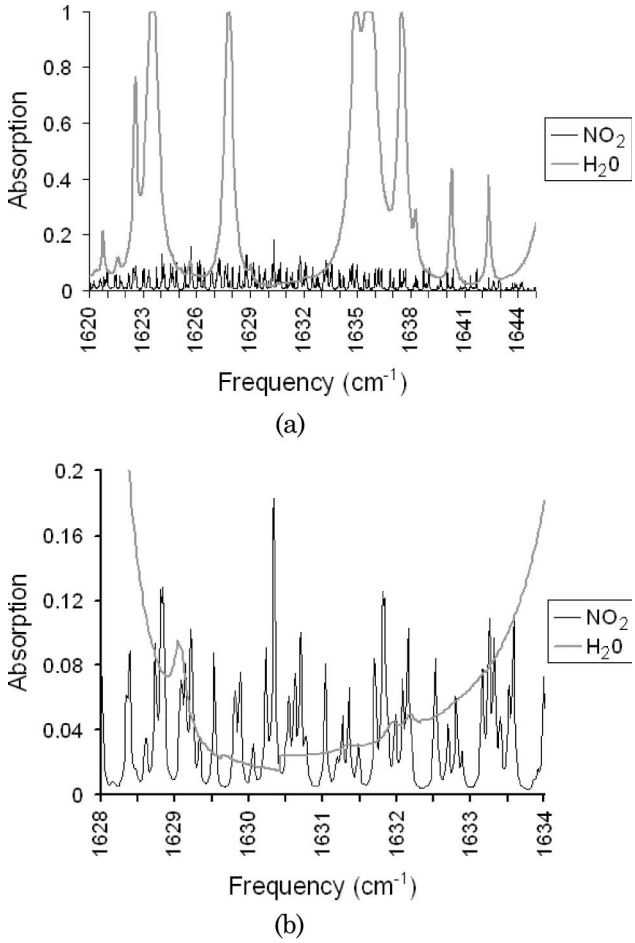

Fig. 3. (a) Simulated NO_2 spectrum (50 ppm at 200 mbar) for the R-branch between 1620 and 1645 cm^{-1}. Overlaid onto the spectrum are the water lines that match typical conditions in the mid-latitude United States during the summer months. This spectrum was used to select a region with a strong dense NO_2 spectrum that was free from interference due to water lines. (b) Close-up of the region that was recorded and integrated.

3. Results and Discussion

We first determined the sensitivity of the apparatus using WMS of a single absorption feature by recording the second harmonic WMS of the NO_2 doublet at 1631.02 cm^{-1} (at a pressure of 110 ± 10 mbar and concentration of 2.5 ppm). This feature was selected because it is both a typically strong feature in the R-band (intensity $\sim 10^{-19}$ cm/molecule) and relatively well separated from neighboring absorption features. The doublet results from the transitions between the $(0\,0\,1) - (19\,2\,17)$ and $(0\,0\,0) - (18\,2\,16)$ levels; the individual lines are located at 1631.023 and 1631.026 cm^{-1} [note that the $(\nu_1\,\nu_3\,\nu_3) - (N\,K_a\,K_c)$ level notation is used] [12]. The lines' separation of 0.003 cm^{-1} is narrower than the 0.023 cm^{-1} FWHM of the individual lines at 110 mbar, and results in a single observed absorption feature. The recorded second harmonic WMS spectrum is shown in Fig. 4(a) (note that the second harmonic signals from other nearby multiplets can be seen at 1630.8 cm^{-1} and in the region above 1631.2 cm^{-1}). We compare the amplitude of the second harmonic WMS from the 1631.02 doublet to the noise spectrum seen in

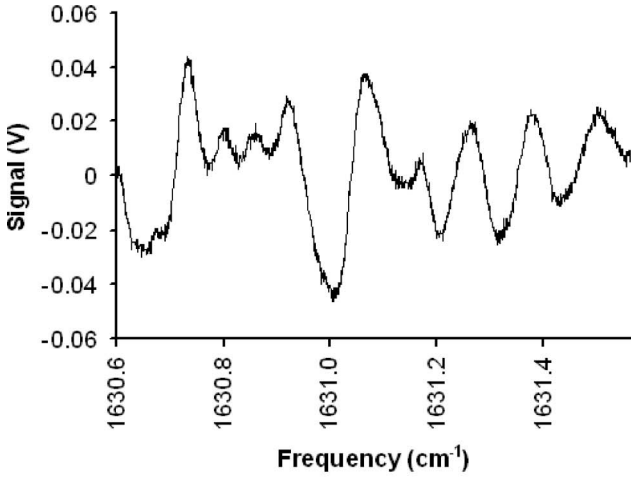

(a)

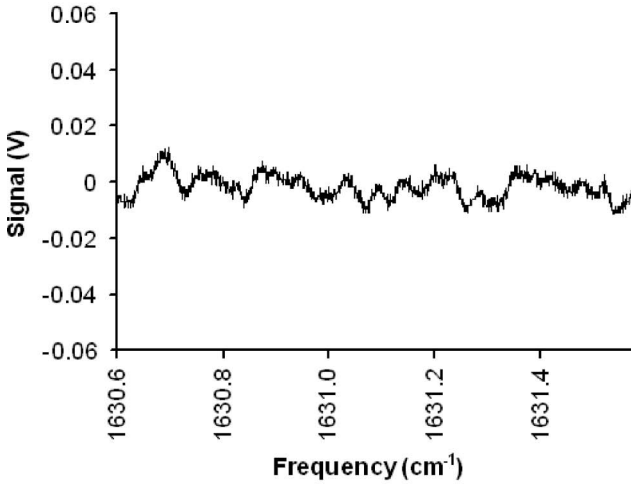

(b)

Fig. 4. (a) Second harmonic WMS signal of the absorption spectrum of the doublet at 1629.52 cm^{-1}. The NO_2 concentration was 2.5 ± 0.38 ppm at a pressure of 110 ± 10 mbar. The second harmonic signals from other nearby multiplets can also be seen at 1630.1 cm^{-1} and in the region above 1630.7 cm^{-1}. (b) The noise content is shown for the same region and was obtained under the same operating conditions, but with an empty cell.

Fig. 4(b) (which was obtained under the same operating conditions, but with an empty cell), and find that the signal-to-noise ratio for the doublet is approximately 10. The sensitivity of the apparatus determined using the second harmonic WMS signal from a single absorption feature is, therefore, approximately 250 ppb.

To measure the sensitivity that may be obtained by integrating the multiline wavelength modulation spectra recorded over a tuning range, we recorded the second harmonic WMS spectra for five concentrations of NO_2 (4.5, 2.5, 1, 0.5, and 0.27 ppm), at a pressure of 110 ± 10 mbar. The spectra were recorded in the frequency range from 1629.5 to 1633.9 cm^{-1}. The concentrations were selected to ensure that the data were in the weakly absorbing regime (i.e., the absorption of the strongest line was less than 5%). The absolute value of the data from each spectrum were then summed to yield the integrated second harmonic WMS signal W_T for the corresponding concentration. Each of these values is subtracted from the integrated second harmonic WMS signal recorded for an evacuated sample cell; this results in the area under the absolute value of the WMS spectrum for the corresponding concentration (we refer to this as the total second harmonic WMS signal for a given concentration). Figure 5(a) shows a plot of the total second harmonic WMS signal versus concentration, as well as a weighted linear least-squares fit of these data (the y axis is given in arbitrary units). Figure 5(b) uses an expanded scale to display the low concentration portion of the data.

The instrument's sensitivity is determined from the y intercept of the linear fit. We take the y-intercept value of −0.2025 total second harmonic WMS units and divide it by the slope of the fit

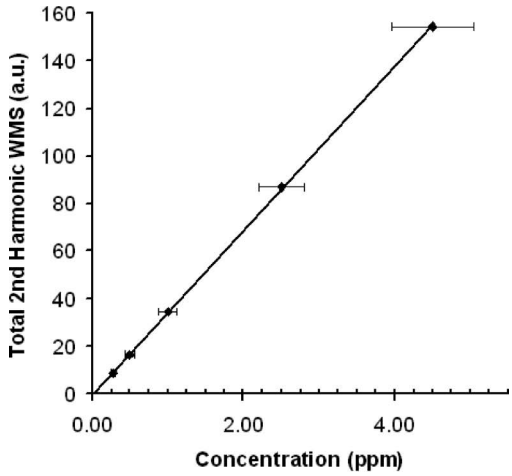

(a)

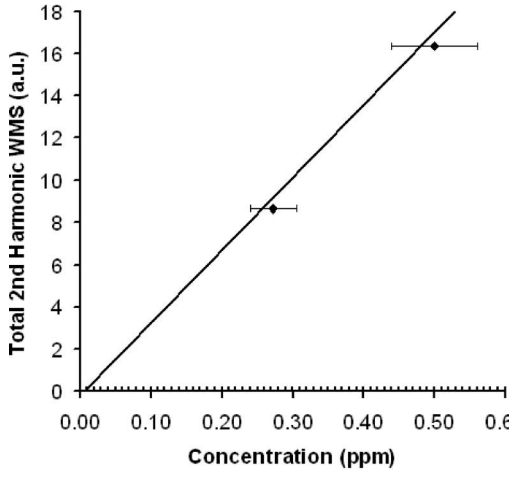

(b)

Fig. 5. (a) Total second harmonic WMS signal versus concentration plot. The expected linear relationship between the integrated second harmonic WMS signal of the various concentrations is seen. The y intercept is used to determine the sensitivity of detection. (b) Expanded scale of the low concentration region is employed to clearly display the low concentration data points.

(34.46 total second harmonic WMS units/ppm) to obtain a sensitivity of the order of 6 ppb. This shows a factor of 40 improvement in sensitivity compared to WMS of a single line conducted using the same apparatus. It should also be noted that this shows a factor of 20 improvement in sensitivity over our previously reported work with multiple-line integrated absorption spectroscopy [11].

One should note that, even though the NO_2 mixtures were generated using zero air (a dehumidified air mixture), our results are representative of what one would expect if the NO_2 was in ambient air. This is a result of our experimental layout, where the laser beam travels through approximately 1 m of ambient air before reaching the cell. In fact, it should be noted that the multiple-line integrated WMS technique is less susceptible to interference from water lines compared to other absorption-based techniques. This is because achieving sensitivities on the ppb level using a single line requires long path lengths (tens or hundreds of meters), resulting in a saturation and broadening of the water lines present in the sample, which can prevent the observation of NO_2 spectra unless one first takes preparatory steps, such as dehumidifying the sample.

4. Conclusion

We describe and demonstrate a technique that enhances the sensitivity of a spectrometer for trace gas detection by integrating the absolute value of the wavelength modulation spectra from multiple spectral lines. In particular, we use WMS of a single line with a tunable, CW quantum cascade laser and a short-path absorption cell to detect low concentrations of NO_2 with a sensitivity of approximately 250 ppb. By integrating the second harmonic WMS spectra over multiple lines with the same experimental apparatus, we detect concentrations of NO_2 with a sensitivity of the order of 6 ppb, demonstrating a factor of 40 improvement in the instrument's sensitivity. We feel that this technique may be useful for the detection of polyatomic species, such as NO_2, that have dense rotational–vibrational spectra over a relatively compact frequency range. Although this experiment was conducted using a quantum cascade laser with a wide mode-hop-free tuning range, it could be employed with any tunable laser source that is capable of tuning across multiple transitions of the target species. Additional improvements to the sensitivity may be achieved by using this technique with long optical path-length apparatus, such as a Herriot cell or integrated cavity output spectroscopy, and should enable sensitivity in the tens of ppt.

References

1. United States Environmental Protection Agency, "National air quality status and trends through 2007," EPA-454/R-08-006 (2008).
2. J. Hildenbrand, J. Herbst, J. Wöllenstein, and A. Lambrecht, "Explosive detection using infrared laser spectroscopy," Proc. SPIE **7222**, 72220B (2009).
3. T. H. Risby and S. F. Solga, "Current status of clinical breath analysis," Appl. Phys. B **85**, 421–426 (2006).
4. A. A. Kosterev, R. F. Curl, F. K. Tittel, M. Rochat, M. Beck, D. Hofstetter, and J. Faist, "Chemical sensing with pulsed QC-DFB lasers operating at 6.6 μm," Appl. Phys. B **75**, 351–357 (2002).
5. F. K. Tittel, Y. Bakhirkin, A. Kosterev, and G. Wysocki, "Recent advances in trace gas detection using quantum and interband cascade lasers," Rev. Laser Eng. **34**, 275–282 (2006).
6. G. Wysocki, R. Curl, F. Tittel, R. Maulini, J. Billiard, and J. Faist, "Widely tunable mode-hop free external cavity quantum cascade laser for high resolution spectroscopic applications," Appl. Phys. B **81**, 769–777 (2005).
7. A. Karpf and G. N. Rao, "Absorption and wavelength modulation spectroscopy of NO_2 using a tunable, external cavity continuous wave quantum cascade laser," Appl. Opt. **48**, 408–413 (2009).
8. J. Reid and D. Labrie, "Second-harmonic detection with tunable diode lasers—comparison of experiment and theory," Appl. Phys. B **26**, 203–210 (1981).
9. G. N. Rao, C. Gudipaty, and D. Martin, "Higher harmonic detection employing wavelength modulation spectroscopy and near infra-red diode lasers: an undergraduate experiment," Am. J. Phys. **77**, 821–825 (2009).
10. J. M. Hollas, *High Resolution Spectroscopy, Second Edition* (Wiley 1998).
11. A. Karpf and G. N. Rao, "Enhanced sensitivity for the detection of trace gases using multiple line integrated absorption spectroscopy," Appl. Opt. **48**, 5061–5066 (2009).
12. L. S. Rothman, D. Jacquemart, A. Barbe, D. C. Benner, M. Birk, L. R. Brown, M. R. Carleer, C. Chackerian Jr., K. Chance, L. H. Coudert, V. Dana, V. M. Devi, J.-M. Flaud, R. R. Gamache, A. Goldman, J.-M. Hartmann, K. W. Jucks, A. G. Maki, J.-Y. Mandin, S. T. Massie, J. Orphal, A. Perrin, C. P. Rinsland, M. A. H. Smith, J. Tennyson, R. N. Tolchenov, R. A. Toth, J. Vander Auwera, P. Varanasi, and G. Wagner, "The HITRAN 2004 molecular spectroscopic database," J. Quant. Spectrosc. Radiat. Transfer **96**, 139–204 (2005).
13. C. N. Mikhailenko, Yu. L. Babikov, and V. F. Golovko, "Information-calculating system spectroscopy of atmospheric gases. The structure and main functions," Atmos. Oceanic Opt. **18**, 685–695 (2005).
14. G. Hancock, J. H. van Helden, R. Peverall, G. A. D. Ritchie, and R. J. Walker, "Direct and wavelength modulation spectroscopy using a cw external cavity quantum cascade laser," Appl. Phys. Lett. **94**, 201110, doi: 10.1063/1.3141521 (2009).
15. G. Schilt, L. Thévenaz, and P. Robert, "Wavelength Modulation Spectroscopy: combined frequency and intensity modulation," Appl. Opt. **42**, 6728–6738 (2003).
16. H. Li, G. B. Rieker, X. Liu, J. B. Jeffries, and R. K. Hanson, "Extension of wavelength modulation depth for diode laser absorption measurements in high-pressure gases," Appl. Opt. **45**, 1052–1061 (2006).
17. National Aeronautic and Space Administration, "Earth fact sheet—terrestrial atmosphere," http://nssdc.gsfc.nasa.gov/planetary/factsheet/earthfact.html.
18. E. De Tommasi, G. Casa, and L. Gianfrani, "High precision determinations of NH_3 concentration by means of diode laser spectrometry at 2.005 μm," Appl. Phys. B **85**, 257–263 (2006).
19. E. Burkhard and J. Schwab, "Ambient gaseous ammonia: evaluation of continuous measurement methods suitable for routine deployment—final report" (New York State Energy Research and Development Authority, 2008).
20. National Oceanic and Atmospheric Administration, "Average relative humidity," http://lwf.ncdc.noaa.gov/oa/climate/online/ccd/avgrh.html.